JACS
JOURNAL OF THE AMERICAN CHEMICAL SOCIETY
Article
pubs.acs.org/JACS

Dimyristoyl Phosphatidylcholine: A Remarkable Exception to α-Tocopherol's Membrane Presence

Drew Marquardt,*[,†] Justin A. Williams,[‡] Jacob J. Kinnun,[‡] Norbert Kučerka,[¶] Jeffrey Atkinson,[§] Stephen R. Wassall,[‡] John Katsaras,[∥,⊥,†,#] and Thad A. Harroun*[,†]

[†]Department of Physics, Brock University, St. Catharines, Ontario L2S 3A1, Canada
[‡]Department of Physics, Indiana University Purdue University Indianapolis, Indianapolis, Indiana 46202, United States
[¶]National Research Council, Canadian Neutron Beam Centre, Chalk River, Ontario K0J 1J0, Canada
[§]Department of Chemistry, Brock University, St. Catharines, Ontario L2S 3A1, Canada
[∥]Oak Ridge National Laboratory, Oak Ridge, Tennessee 37831, United States
[⊥]Joint Institute for Neutron Sciences, Oak Ridge, Tennessee 37831, United States
[#]Department of Physics, University of Tennessee, Knoxville, Tennessee 37996, United States

ABSTRACT: Using data obtained from different physical techniques (i.e., neutron diffraction, NMR and UV spectroscopy), we present evidence which explains some of the conflicting and inexplicable data found in the literature regarding α-tocopherol's (aToc's) behavior in dimyristoyl phosphatidylcholine (di-14:0PC) bilayers. Without exception, the data point to aToc's active chromanol moiety residing deep in the hydrophobic core of di-14:0PC bilayers, a location that is in stark contrast to aToc's location in other PC bilayers. Our result is a clear example of the importance of lipid species diversity in biological membranes and importantly, it suggests that measurements of aToc's oxidation kinetics, and its associated byproducts observed in di-14:0PC bilayers, should be reexamined, this time taking into account its noncanonical location in this bilayer.

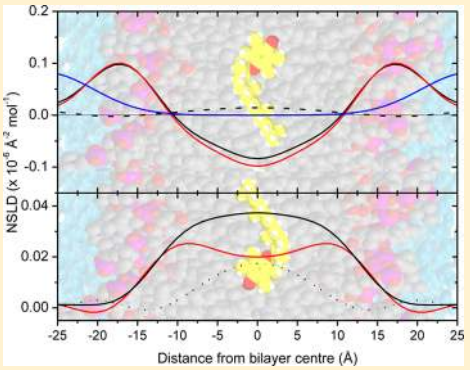

INTRODUCTION

Even though it was discovered more than 90 years ago by Evans and Bishop,[1] vitamin E's role in biological systems remains controversial. In mammals, vitamin E deficiency has been associated with sterility, muscle disease, degeneration of the central nervous system and peripheral nerves, and reduced life spans of human red blood cells.[2,3] Commonly thought as a single molecule, vitamin E comprises a family of eight related molecules, collectively known as tocopherols and tocotrienols, with each group made up of different homologues (i.e., α, β, γ, and δ) with specific substitutions to their chromanol rings. For the most part, dietary vitamin E is composed of α- and γ-tocopherol, but only α-tocopherol (aToc) (Figure 1) is retained by the human body.[4] Vitamin E is commonly thought to be an effective fat soluble antioxidant, and as such, is commonly used as a preservative by the cosmetic and food industries. Despite its industrial utility, aToc's *in vivo* role at the molecular level has remained elusive.

There are many conflicting reports regarding aToc's biological function. For example, Traber and Atkinson reported that all observations regarding aToc's *in vivo* mechanism of action were consistent with its role as a potent, lipid-soluble antioxidant.[5] However, using the same data Azzi argued that its physiological concentration levels are insufficient for it to effectively act as an antioxidant.[6] To a great extent, this ambiguity regarding aToc's physiological role has been perpetuated by inconclusive, and sometimes, conflicting experimental data.

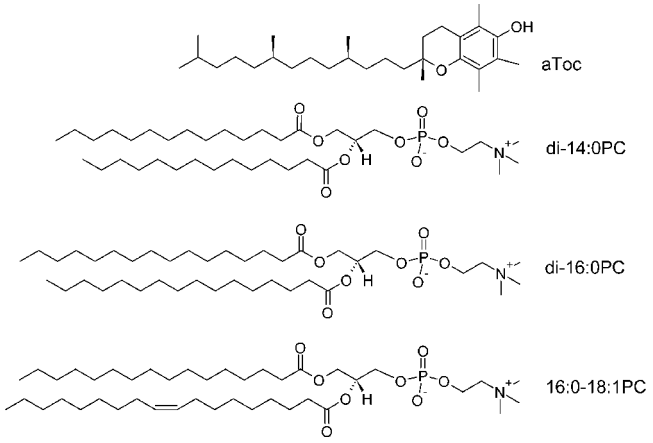

Figure 1. Structures of α-tocopherol (aToc), 1,2-dimyristoyl-*sn*-glycero-3-phosphocholine (di-14:0PC), 1,2-dipalmitoyl-*sn*-glycero-3-phosphocholine (di-16:0PC), and 1-palmitoyl-2-oleoyl-*sn*-glycero-3-phosphocholine (16:0-18:1PC).

Received: August 9, 2013
Published: December 5, 2013

   dx.doi.org/10.1021/ja408288f | *J. Am. Chem. Soc.* 2014, 136, 203−210

Over the years, a significant number of biophysical studies using model systems has contributed to our knowledge of aToc in membranes. Frequently, however, much of this research used saturated phosphatidylcholine lipid bilayers, despite the fact that they do not undergo lipid peroxidation. For decades, biophysicists have used di-14:0PC (dimyristoyl phosphatidylcholine - di-14:0PC) (Figure 1), a lipid with saturated myristoyl (14:0) chains at the sn-1 and sn-2 positions as a biological mimic. Its popularity as a model membrane system can be attributed to the fact that it is stable, inexpensive, and easy to obtain. As a result, di-14:0PC has been used to examining the location, behavior, and antioxidant properties of aToc in biomimetic membranes.[7−11]

Di-16:0PC (dipalmitoyl phosphatidylcholine - di-16:0PC) (Figure 1) is similar to di-14:0PC in structure and popularity as a membrane model. In a landmark study, Tardieu et al.[12] described a variety of then newly observed lamellar and nonlamellar phases formed by di-14:0PC and di-16:0PC lipid−water systems, including the much-studied gel and rippled bilayers,[13] and biologically relevant liquid crystalline bilayers.[14] In low-temperature gel phase membranes, lipid hydrocarbon chains are almost fully extended and well-ordered within the two-dimensional plane of the bilayer.[15−17] In contrast, however, the hydrocarbon chains of liquid crystalline bilayers are in a melted state, and hence, the ordering of molecules within each layer is liquid-like. Apart from their (i.e., di-14:0PC and di-16:0PC) main gel−liquid crystalline phase transitions being separated by about 20 °C (di-16:0PC has longer acyl chains), morphologically there is very little difference between these two model membrane systems.

1-Palmitoyl-2-oleoyl phosphatidylcholine (16:0-18:1PC) (Figure 1) is one of the most abundant phospholipids in eukaryotic cells. Similar to di-16:0PC, 16:0-18:1PC also undergoes a gel−liquid crystalline phase transition; however, it takes place at a much lower temperature than the two aforementioned lipid systems. Despite having one unsaturated hydrocarbon chain, aToc's location in 16:0-18:1PC bilayers was recently shown to be no different than what was observed in di-16:0PC bilayers.[18]

A natural extension of work examining the physical properties of pure lipid bilayers has been studies that determine the location of biomolecules in model membrane systems. For example, the chromanol ring of brominated δ-tocopherol was found localized in the vicinity of the glycerol backbone-headgroup region of di-16:0PC bilayers, with and without cholesterol.[19] EPR studies of PC lipids with increasing levels of unsaturation, including di-14:0PC, found that aToc perturbed the molecular organization of di-14:0PC bilayers much more than any other bilayer system.[9] Recently, we determined the location of aToc in different lipid bilayers, and concluded that its nominal upright orientation was the result of steric interactions taking place at its phytyl tail and chromanol headgroup.[18] In effect, the data demonstrated that aToc's location and antioxidant activity are precisely correlated with the depth of its sacrificial hydroxyl (located on its chromanol ring) within the lipid matrix.

Here we report aToc's unexpected location in di-14:0PC bilayers, a location which may reconcile decades of conflicting results. Using neutron scattering and multibilayer stacks of di-14:0PC containing 10 mol % aToc, we have found that aToc sequesters itself in the bilayer's center, not unlike what was previously observed with cholesterol in bilayers wtih lipids containing polyunsaturated fatty acid (PUFA) acyl chains.[20,21] Solid state ^{2}H NMR measurements of aToc's effect on acyl chain order of di-14:0PC bilayers, also support this finding. The present result is in marked contrast to all other results regarding the vitamin's orientation in model membranes.

RESULTS

Neutron Diffraction. One-dimensional (1D) neutron scattering length density (NSLD) profiles of di-14:0PC bilayers, with and without aToc, were determined using oriented multibilayer stacks adsorbed to the surface of a single crystal Si substrate. Multibilayers were hydrated in a 92% relative humidity (RH) environment at 28 °C, inducing the formation of biologically relevant liquid crystalline bilayers. When interrogated by a monochromatic beam of neutrons (λ = 2.37 Å), between 4 and 6 quasi-Bragg peaks were observed (Figure 2) -

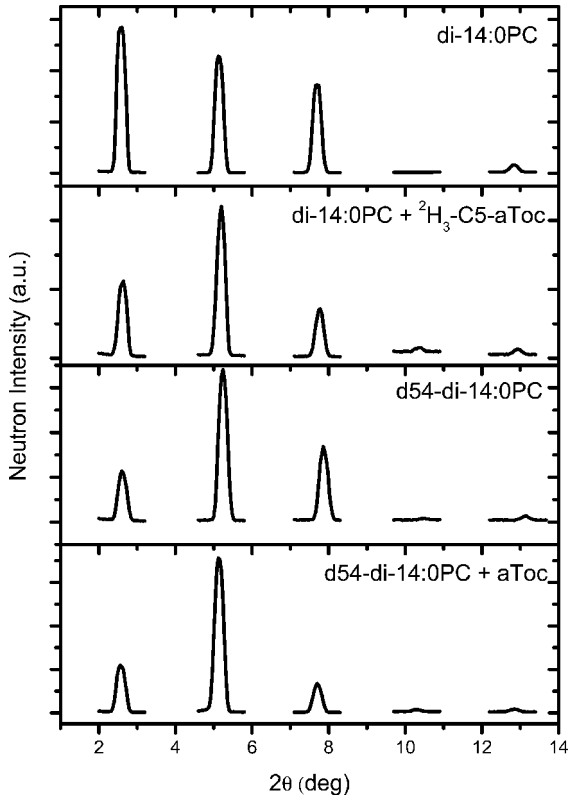

Figure 2. Uncorrected diffraction intensity as a function of the scattering angle 2θ, for di-14:0PC + aToc, di-14:0PC + $^2H_3$ − C5-aToc, [$^2H_{54}$]-di14:0PC, and [$^2H_{54}$]-di14:0PC + aToc all hydrated with 8% ^2H_2O.

the number of observed peaks depended on the percent ^2H_2O making-up the hydrating water solution. The lamellar repeat spacing (d) of bilayers with and without aToc was 53 Å. The bilayer thickness (phosphate−phosphate distance) was ~37 Å, and the hydrocarbon thickness was ~24 Å. These three bilayer parameters, namely d-spacing, bilayer thickness and hydrocarbon thickness are in good agreement with those determined by Kučerka et al. for liquid crystalline di-14:0PC bilayers.[14,22]

A first comparison was made between protiated di-14:0PC with 10 mol % protiated aToc or $^2H_3$−C5-aToc. Figure 3A shows the one-dimensional (1D) NSLD profiles of liquid crystalline di-14:0PC bilayers containing the labeled (black curve) and unlabeled (red curve) aToc. The difference 1D NSLD (dashed line) between the two samples is the averaged mass distribution (location) of the C5 methyl on the chromanol ring within the bilayer. From NSLD, it is clear that the vitamin's chromanol group resides in the middle of di-14:0PC bilayers (Figure 3A), a

dx.doi.org/10.1021/ja408288f | J. Am. Chem. Soc. 2014, 136, 203−210

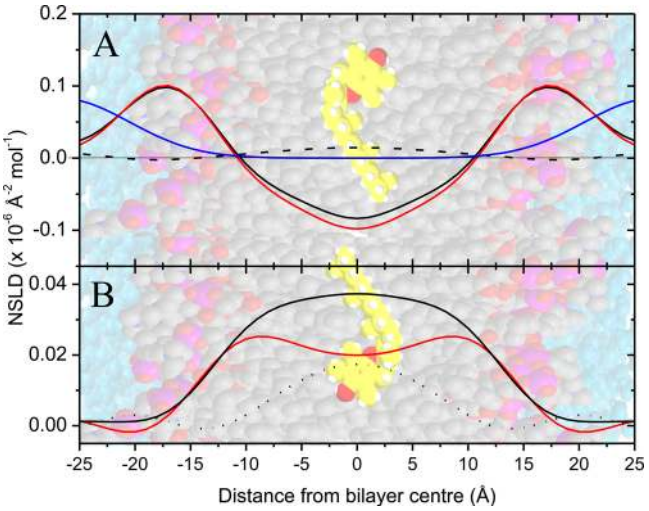

Figure 3. (A) 1D NSLD profile of a di-14:0PC bilayer with 10 mol % of either labeled (black curve) or unlabeled (red curve) aToc. The dashed curve is the difference NSLD profile showing the mass distribution of aToc's C5 methyl deuterium label. The blue curve is the water distribution across the bilayer. (B) The hydrocarbon chain distribution profiles for pure [$^2H_{54}$]-di14:0PC (black) and [$^2H_{54}$]-di14:0PC with 10 mol % protiated aToc (red), with the dashed line representing the difference in NSLD between the two distributions. The center of the difference distribution shows an overall NSLD decrease as a result of the protiated aToc locating in the bilayer center.

result which is not dissimilar from that of cholesterol in PUFA membranes.[20,21]

A second comparison was made between perdeuterated di-14:0PC (d54-di-14:0PC) bilayers with and without protiated aToc. Figure 3 shows comparison and difference (dashed line) NSLD profiles of d54-di-14:0PC bilayers, with and without protiated aToc. The NSLD is dominated by the signal from the deuterated acyl chains. In the case of protiated hydrocarbon chains one commonly sees a dip at the center of the bilayer, consistent with the negative scattering length from CH_3. However, with the hydrogens on the acyl chain replaced with deuterium, the data do not show a dip at the bilayer center but instead show the positive scattering length density associated with CD_3 groups. The addition of protiated aToc clearly reduces the NSLD amplitude in the center of the bilayer. This is due to the fact that aToc resides entirely at the bilayer center and is not simply flipped upside-down. The current results are in contrast to those obtained from recently studied PC bilayers, where aToc's chromanol and phenolic groups were found located in the upright orientation, fixed for the most part in the vicinity of the glycerol backbone regardless of acyl chain unsaturation (bilayer unsaturation ranged from fully saturated di-16:0PC to the omega-6 PUFA di-20:4PC), as shown in Figure 4.[18]

It therefore stands to reason that the difference between aToc's location in di-14:0PC and the other lipids studied could have profound implications with regard to its role as a free radical scavenger. For example, using a combination of neutron scattering and chemical reaction data, Marquardt et al. (2013) have clearly shown that small differences in aToc's location in a membrane are directly related to its ability to protect the phospholipids from free radicals and/or the termination of acyl-radical oxidation chain reactions. Specifically, it was determined that aToc is best able to protect against waterborne reactive oxygen species when situated higher in the membrane (closer to the lipid−water interface), a location where it is most able to deal with reactive species produced by Fenton chemistry. On the other hand, when located slightly lower in the membrane, aToc can intercept and terminate acyl chain peroxyl radicals which snorkle to the membrane's surface.[18]

^{2}H NMR. To compare the effect of aToc on the molecular organization of different bilayers, solid state ^{2}H NMR spectra were collected using aqueous multilamellar dispersions of

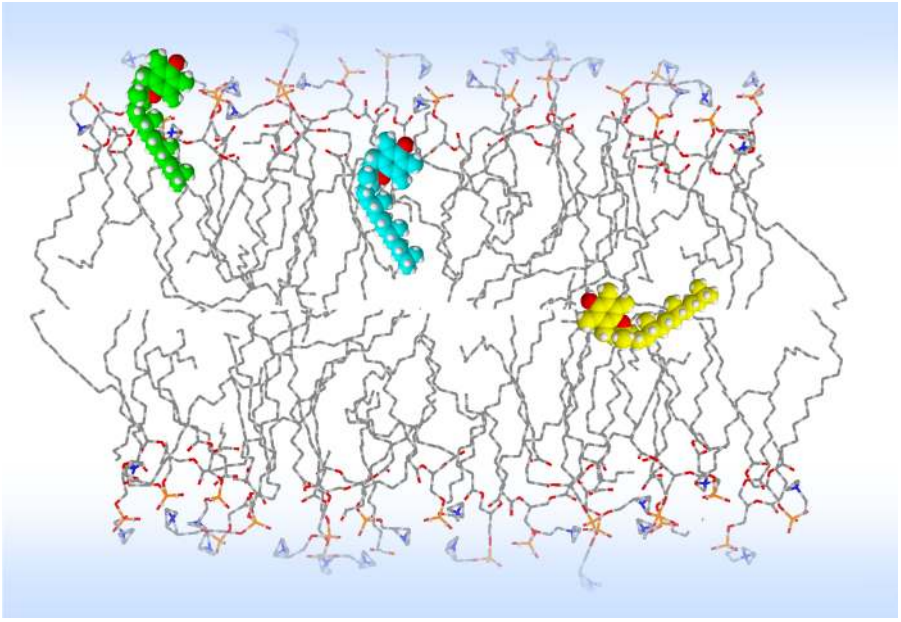

Figure 4. A schematic representation of aToc locations in different PC bilayers. The green aToc shows its location in the vicinity of the PC headgroups when in di-16:0PC, 16:0-18:1PC, and PUFA di-20:4PC bilayers. The cyan aToc shows the vitamin's location in di-18:1PC and 16:0−20:4PC bilayers. In these bilayers, aToc resides near the lipid−water interface (i.e., glycerol backbone).[18] Based on the current data, the yellow aToc shows the molecule's location in the center of di-14:0PC bilayers. Its exact orientation (upside-down or lengthwise) is unknown; only the chromanol location is known at this point.

dx.doi.org/10.1021/ja408288f | J. Am. Chem. Soc. 2014, 136, 203−210

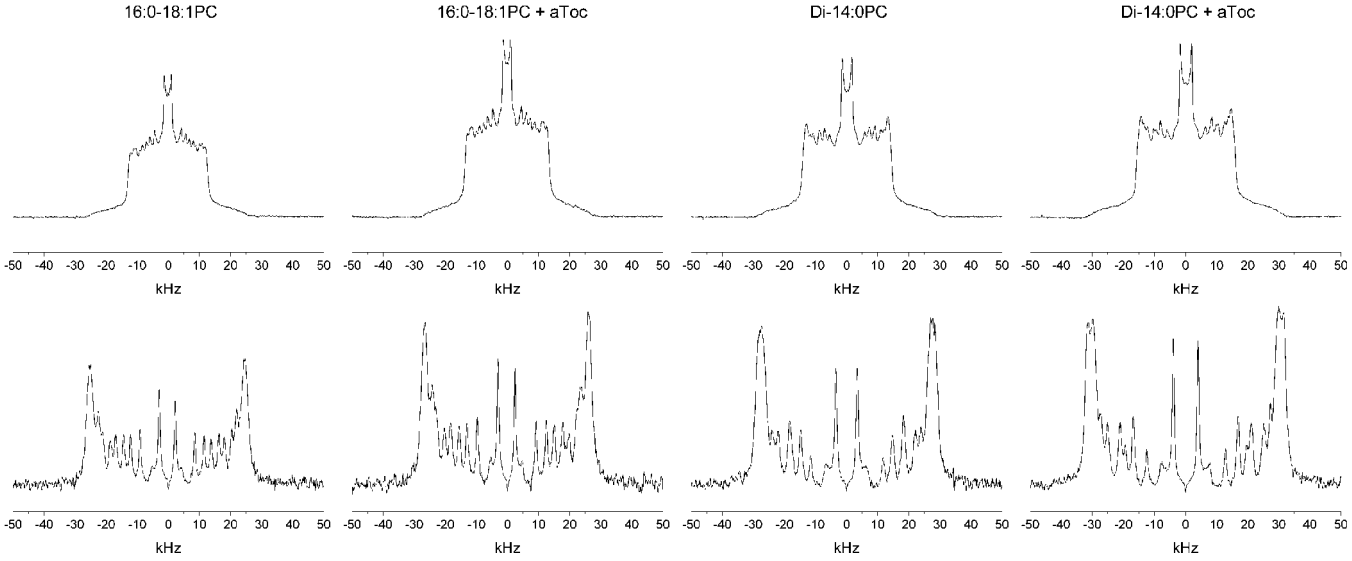

Figure 5. ^{2}H NMR spectra for 50 wt % [$^2H_{31}$]-16:0-18:1PC and 14:0-[$^2H_{27}$]-14:0PC dispersions in 50 mM Tris buffer (pH 7.5) with and without 10 mol % aToc. Top spectra are the conventional powder patterns for each sample, and bottom spectra are the FFT depaked spectra.

[$^2H_{31}$]-16:0-18:1PC and 14:0-[$^2H_{27}$]-14:0 PC with and without 10 mol % aToc at 30 °C (Figure 5). The spectra in the upper row are powder patterns obtained by conventional FFT, and consist of a superposition of signals from bilayers in a spherically symmetrical distribution of orientations relative to the magnetic field. In each case, there are well-defined edges at ~± 15 kHz, which correspond to the plateau region of almost constant order in the upper portion of the perdeuterated chain, while individual peaks within the spectrum arise from the less ordered methylenes in the lower part of the chain, with the central pair of NMR peaks being the result of a highly disordered terminal methyl group.[23] The corresponding FFT depaked spectra[24] that are representative of an aligned multilayer sample are plotted in the lower row. They consist of an outermost composite doublet produced by the plateau region of similarly ordered methylenes in the upper portion of the chain, and five to six well-resolved doublets with progressively less splitting, due to the disordered methylenes and terminal methyl in the lower portion of the chain. The splitting $\Delta\nu(\theta)$ of the doublets relates to the order parameter S_{CD} according to

$$\Delta\nu = \frac{3}{4}\left(\frac{e^2qQ}{h}\right)|S_{CD}|P_2(\cos\theta) \quad (1)$$

where (e^2qQ/h) = 168 kHz is the quadrupolar coupling constant, $P_2(\cos\theta)$ is the second-order Legendre polynomial, and $\theta = 0°$ is the angle the bilayer normal makes with the magnetic field.

Inspection of the innermost pair of peaks, which are attributed to the terminal methyl group in the depaked spectra, show aToc significantly affecting the molecular motions taking place in the center of 14:0-[$^2H_{27}$]-14:0PC bilayers. (Figure 6). In contrast, only a very small increase in splitting, from 5.1 to 5.4 kHz and equivalent to an increase of 0.001 in order parameter, is observed for the terminal methyl group of the sn-1 chain in [$^2H_{31}$]-16:0-18:1PC bilayers upon the incorporation of aToc (Figure 6, top). Similar behavior has been previously seen in previous ^{2}H NMR work on [$^2H_{31}$]-16:0-18:1PC[25] and PC-d31, an analogue prepared from egg PC with [$^2H_{31}$]-16:0 acid substituted at the sn-2 position.[26] In marked contrast, addition of aToc produces a much larger increase in splitting from 6.8 to 8.0 kHz, equivalent to an increase of 0.005 in order parameter, for the terminal

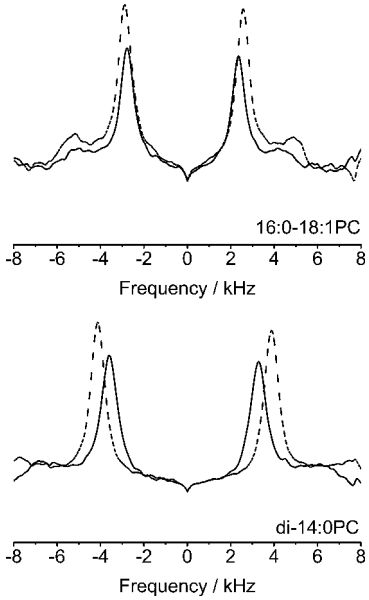

Figure 6. Depaked spectra of the terminal methyl groups from [$^2H_{31}$]-16:0-18:1PC and 14:0-[$^2H_{27}$]-14:0PC bilayers with and without 10 mol % aToc. The effect aToc has on the terminal methyl group is reflected by the increase in splitting of the doublet due to C^2H_3. Solid lines are lipid spectra in the absence of aToc, while dashed lines are those of bilayers with aToc.

methyl group of the sn-2 chain in 14:0-[$^2H_{27}$]-14:0PC bilayers (Figure 6, bottom). This result is consistent with the neutron scattering data that places the rigid chromanol group at the center of the di-14:0PC bilayer, where it is expected to restrict lipid chain motion appreciably, as opposed to [$^2H_{31}$]-16:0-18:1PC bilayers, where the chromanol group would cause less effect at the bilayer center, as it resides at the aqueous surface.

The difference that aToc exerts on the molecular organization of 14:0-[$^2H_{27}$]-14:0PC vs [$^2H_{31}$]-16:0-18:1PC bilayers is elaborated by smoothed profiles of the order parameter (Figure 7). They were generated from the depaked spectra on the basis of the integrated intensity, assuming monotonic variation toward the disordered terminal methyl group.[27] It should be noted,

dx.doi.org/10.1021/ja408288f | J. Am. Chem. Soc. 2014, 136, 203−210

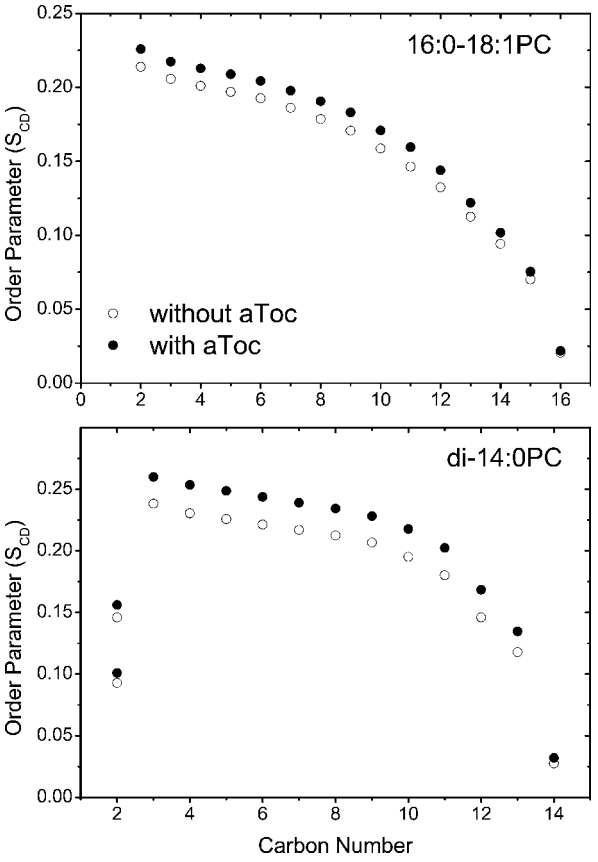

Figure 7. Smoothed order parameter profiles for (top) [$^2H_{31}$]-16:0-18:1PC (POPC) and (bottom) 14:0-[$^2H_{27}$]-14:0PC (DMPC) without (open circle) and with (filled circle) 10 mol % aToc at 30 °C.

however, that this procedure cannot be applied to the C2 position in the sn-2 chain of 14:0-[$^2H_{27}$]-14:0 PC, because conformational constraints imposed by the glycerol backbone render the two deuterons motionally inequivalent. As such, the order parameters were assigned with reference to measurements using selectively deuterated phospholipids.[28] As can be seen, apart from the C2 position in 14:0-[$^2H_{27}$]-14:0PC bilayers, order varies slowly in the upper portion of the chain (plateau region) before decreasing rapidly toward the terminal methyl group, in the lower portion, for both systems with and without aToc. This general form of profile is characteristic of liquid crystalline phospholipid bilayers.[29] Order is elevated throughout the profile following the addition of aToc, which agrees with earlier studies.[18,25,26] The increase is greater for 14:0-[$^2H_{27}$]-14:0PC (11%) than [$^2H_{31}$]-16:0-18:1PC (7%), which is reflected in the average order parameters $\overline{S}_{CD}$ (Table 1) calculated from the profiles, and measured from the first moment M_1 of the powder pattern spectra[23] via

$$M_1 = \frac{\pi}{\sqrt{3}}\left(\frac{e^2qQ}{h}\right)|\overline{S}_{CD}| \quad (2)$$

Significantly, there is a much greater increase in order near the middle of 14:0-[$^2H_{27}$]-14:0 PC compared to [$^2H_{31}$]-16:0-18:1PC. Order parameter ratios in the presence of aToc relative to the pure lipid reveal that, whereas order is uniformly higher (6−8%) throughout the entire chain in [$^2H_{31}$]-16:0-18:1PC, the increase in order in [$^2H_{31}$]-16:0-18:1PC, due to aToc's presence becoming progressively greater along the chain, is greatest (16%) at the terminal methyl end (Figure 8). The observation from the

Table 1. Average Order Parameters Calculated from Powder Pattern and Depaked Data for [$^2H_{31}$]-16:0-18:1PC and 14:0-[$^2H_{27}$]-14:0PC Bilayers with and without 10 mol % aToc at 30 °C[a]

sample	$\overline{S}_{CD}$ measrd.	$\overline{S}_{CD}$ calcd
16:0-18:0PC	0.14(5)	0.14(7)
16:0-18:0PC + aToc	0.15(4)	0.15(8)
di-14:0PC	0.17(0)	0.17(4)
di-14:0PC + aToc	0.18(6)	0.19(3)

[a]The agreement of the values within experimental uncertainty (±1%) serves as validation.

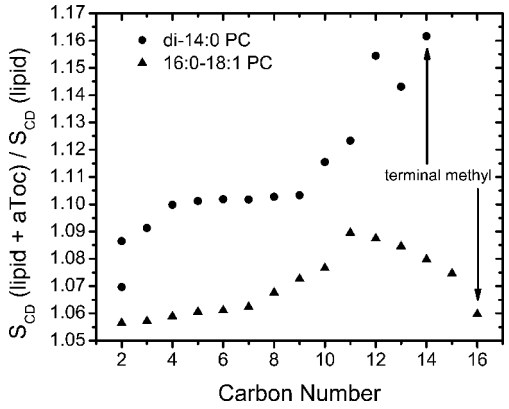

Figure 8. The S_{CD} ratio [$^2H_{31}$]-16:0-18:1 PC bilayers with and without 10 mol % aToc (triangle), and 14:0-[$^2H_{27}$]-14:0PC bilayer with and without 10 mol % aToc (circles) at 30 °C.

neutron scattering experiments that the chromanol group sits at the center of di-14:0PC bilayers, thereby maximally impeding motion in the lower portion of the lipid chain, offers a clear explanation.

While lying between leaflets parallel to the plane of the bilayer is the arrangement presented for aToc in 14:0-14:0PC in Figure 4, it should be acknowledged that other arrangements placing the chromanol in the middle of the bilayer cannot be ruled out. One other possibility is that aToc aligns parallel to phospholipid chains and, unlike the usual upright location, is inverted with its side chain extending toward the bilayer surface in each leaflet. Another possibility, somewhat akin to the situation proposed for *n*-alkanes,[30] has aToc lined up parallel to phospholipid chains but spanning the midplane of the bilayer. Whatever arrangement applies, our results reveal that aToc incorporates anomalously into di-14:0PC bilayers, with its chromanol group residing in the disordered central region of the bilayer.

UV/Vis Oxidation. The proposed new location for aToc in di-14:0PC bilayers presents an interesting challenge. Since aToc's chromanol group resides in the middle of the bilayer, deep in the membrane's hydrophobic core, we would not expect it to interact with free radicals (e.g., O_2^-) diffusing from the water phase. We therefore studied the possibility of the vitamin being oxidized by free radicals generated in bulk water (i.e., water-soluble Fenton chemistry):

$$Fe^{2+} + H_2O_2 \rightarrow Fe^{3+} + OH\bullet + OH^- \quad (3)$$

$$LH + OH\bullet \rightarrow L\bullet + H_2Om \quad (4)$$

or in the bilayer's hydrophobic interior (i.e., hydrophobic AMVN, 2,2′-azobis-(2,4-dimethylvaleronitrile)):[31]

dx.doi.org/10.1021/ja408288f | J. Am. Chem. Soc. 2014, 136, 203−210

$$R - N = N - R \rightarrow 2R\bullet + N_2 \quad (5)$$

$$LH + R\bullet \rightarrow L\bullet + RH \quad (6)$$

similar to the study by Marquardt et al. using di-16:0PC vesicles.[18]

Initiating the peroxidation process in water does not alter aToc's UV/vis spectrum in di-14:0PC vesicles over a period of 8 h (Figure 9), implying that the molecule has no measurable

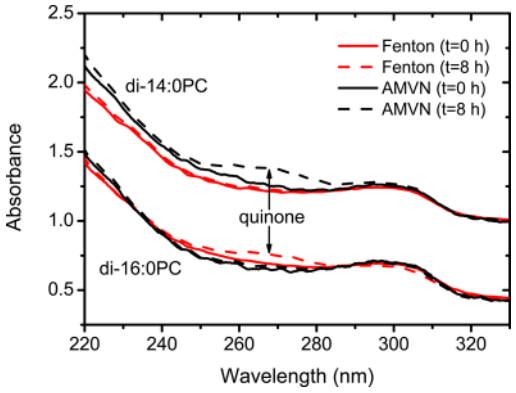

Figure 9. UV/vis spectra of aToc-containing di-14:0PC and di-16:0PC vesicles, with peroxidation initiated in the bilayer's hydrocarbon region (black) and in bulk water (red). Solid lines represent the absorbance prior to the introduction of Fenton reagents to the solution ($t = 0$), and dashed lines represent data taken 8 h after sample exposure. Inset: difference in absorbance between $t = 0$ and $t = 8$. di-16:0PC data from ref 18.

contact with bulk water. This is in contrast to data from di-16:0PC vesicles with aToc, where UV/vis spectra changed in a manner consistent with the vitamin being oxidized and forming tocopherol quinone.[32] On the other hand, the membrane-initiated oxidation process quickly oxidizes aToc in di-14:0PC vesicles, forming tocopherol quinones, clear proof that the vitamin resides in the hydophobic region of the membrane. This effect was not observed in aToc-containing vesicles made from di-16:0PC or 16:0-18:1PC.

DISCUSSION

Over the years, di-14:0PC bilayers have been well characterized using a variety of physical techniques,[14,33,34] and as a result, they've been used to study problems ranging from drug–membrane interactions[35] to the enhancement of cholesterol flip-flop.[36] It is important, however, that because of having fully saturated acyl chains di-14:0PC bilayers are robust and do not require special preparatory environments. On the negative side, the biological relevance of di-14:0PC is questionable due to the low level of 14:0 fatty acid-containing phospholipids in biological systems (e.g., <1% in lipoproteins).[37] Moreover, the fact that di-14:0PC requires no protection against oxidative damage makes it a poor model system to study the *in vivo* antioxidant potential of aToc.

To the best of our knowledge, this is the first report that unambiguously locates aToc in liquid crystalline di-14:0PC bilayers. Knowing its location, we can now make sense of the extensive oxidation data collected by Fukuzawa, where he clearly noted that in pure di-14:0PC liposomes aToc could not be oxidized by waterborne Fe(III)-xanthine oxidase generating O_2^-, unless lipid peroxides were also included.[11] In the only other report looking at di-14:0PC liposomes containing aToc, the vitamin was oxidized only when the entire sample was irradiated by Co-60 γ-rays.[32] This result is consistent with aToc's newly proposed location in di-14:0PC bilayers, as oxidation is not only initiated by free radicals, but also from γ-ray-induced lipid radicals generated in the bilayer's hydrophobic core.

Other studies of aToc-containing di14:0-PC liposomes included as much as 10 mol % stearyl amine or dicetyl phosphate (in order to impart an electric charge to the liposomes). However, aToc concentrations used were in amounts equal or less than additive amounts. It is thus very likely that the additives reoriented the aToc to its nominal upright orientation, where it could be oxidized.[32,38,39] For example, the addition of merely 5 mol % of di-14:0PC to PUFA bilayers caused cholesterol to reorient from the bilayer center to its nominal upright orientation.[36,40] Moreover, molecular dynamics simulations have shown that cholesterol in PUFA bilayers undergoes rapid flip-flop between the two membrane leaflets, but spends a considerable amount of time in the center of PUFA bilayers.[41] That aToc is sequestered in the middle of pure di14:0-PC bilayers contradicts the amphipathic nature of aToc. The fact this occurs in this lipid alone, and can be righted with the inclusion of other lipids species, indicates how, in certain situations, steric interactions can exceed the hydrophobic effect.

There are other studies that have shown aToc being oxidized in different model membranes by waterborne free radicals. Some of these membranes were made from egg yolk PC (abundant in 16:0-18:1PC),[38,42−44] di-16:0PC,[45] 16:0-20:4PC, and 16:0-18:2PC.[46] The data from these studies are all in excellent agreement with the recent report by Marquardt et al.[18] On the other hand, aToc in pure di-14:0PC liposomes can seemingly scavenge waterborne singlet oxygens ($^1O_2$).[11] Singlet oxygen scavenging consists of quenching to a stable triplet $^3O_2$ and an oxidation reaction. Both of these reactions are strongly correlated with the polarity of the environment in which they find themselves. Fukuzawa also noted that aToc has an apparent lower rate constant for $^1O_2$ scavenging when the oxygen is produced in the bilayer's hydrophobic core, as compared to water. It therefore seems that waterborne $^1O_2$ can in fact oxidize aToc in pure di-14:0PC, but a superoxide radical cannot.[11]

At this point we would like to clarify a couple of issues. First, the quenching rate of a singlet oxygen is several orders of magnitude greater than its reaction rate, which was determined by direct oxidation competition with 1,3-diphenylisobenzofuran, and which may itself initiate oxidation. Second, and as noted by Fukuzawa, the concentration distribution of 1,3-diphenylisobenzofuran in a heterogeneous sample precludes the ability to accurately determine rate constants. Taking into account the location of aToc in vesicles versus solution, and even within the vesicles themselves, the difference in rate constants between waterborne and lipid-borne singlet oxygen is almost negligible.[11] We thus suggest that what remains (a rate constant well below that for the same species measured in ethanol) is nothing more than the natural background decay of a singlet oxygen.

Di-14:0PC bilayers have also proven to be inimical with regard to the location of aToc within the membrane. Fukuzawa assigned an almost equal probability of locating the vitamin's chromane ring at the lipid/water interface and the membrane's hydrocarbon core.[11] This conclusion was in part based on data from fluorescence quenching studies, where he surmised that aToc resided in its nominal upright position, with its chromanol ring near the hydrogen belt, but not in the bilayer center,[11] a result which is in good agreement with all membrane systems, except di-14:0PC.[18] The difference between the present data and those

dx.doi.org/10.1021/ja408288f | J. Am. Chem. Soc. 2014, 136, 203−210

by Fukuzawa[11] may be attributed to the fluorescent probes used, which most likely enabled aToc to revert to its nominal upright orientation.[11,47,48] As mentioned, this scenario is not unlike the one of cholesterol in PUFA bilayers, which was discussed in a previous part of this contribution.[36,40]

FT-IR experiments have also shown that the addition of aToc in di14:0-PC bilayers did not affect either the P═O or the C═O stretching modes, implying that the phospholipid's headgroup and glycerol backbone, respectively, did not interact with aToc.[48] However, Villalain and co-workers reported changes to FT-IR spectra when studying di-16:0PC bilayers with aToc.[49] It is understandable, then, that aToc residing in the bilayer's center is sufficiently separated from these functional groups as not to cause any appreciable changes to the aforementioned stretching modes. Moreover, using a combination of NMR and Reichardt's dye polarity measurements, Afri et al. inferred the position of aToc's chromane ring to be in the vicinity of the C-5 to C-7 hydrocarbon chain region of di-14:0PC bilayers, a result closer in agreement with the present neutron data.

Our experiments, as well as those by Fukuzawa, used 10 mol % aToc (a concentration well in excess of physiological concentrations) to provide the necessary experimental signal. We do not expect aToc's location in single-type lipid systems to be concentration dependent. However, in mixed lipid membranes, aToc can potentially phase separate into domains, where the local concentration can rise appreciably. Presently, it is not clear how much localized, increased aToc concentration is taking place until experiments measuring the association constant of aToc with different lipid species are complete.

CONCLUSION

We have presented structural data that rationalize much of the contradictory data found in the literature. Our neutron, ^{2}H NMR, and oxidation assay data unambiguously locate aToc's chromanol moiety in the center of di-14:0PC bilayers. This proposed new location for the vitamin in di-14:0PC membranes explains its inability to be oxidized. Previous data locating the vitamin's chromanol ring at the lipid/water interface of di-14:0PC bilayers are most likely the result of aToc associating with the long-chain fluorescence probes used, enabling it to revert to its nominal upright orientation. This scenario is similar to di-14:0PC causing cholesterol to reorient in PUFA membranes.[36,40]

METHODS

Materials. Phosphatidylcholine lipids were purchased from Avanti Polar Lipids (Alabaster, AL) and used without further purification. After use they were tested for degradation by TLC. Lipids studied were of the form 1-acyl-2-acyl-*sn*-glycero-3-phosphatidylcholine namely, palmitoyl-oleoyl (16:0-18:1PC) and palmitoyl-d_{31}-oleoyl ([$^2H_{31}$]-16:0-18:1PC), dimyristoyl (di-14:0PC), d_{54}-dimyristoyl (d_{54}-di-14:0PC), and myristoyl-myristoyl-d_{27} (14:0-[$^2H_{27}$]-14:0PC). α-[5-$^2H_3$]Tocopherol (aToc-C5d_3) was prepared following a published protocol,[18,50] and D-α-tocopherol (aToc) was purchased from Cole-Parmer (Vernon Hills, IL).

Neutron Diffraction. The methods of sample preparation and neutron diffraction follow those described by.[20,40] All preparations of aligned multilayer samples were carried out in a nitrogen-rich environment. A total of 12 mg of di-14:0PC with 10 mol % aToc was codissolved in chloroform or chloroform−trifluoroethanol (3:1). The solution was deposited on a silicon single-crystal substrate, and the solvent was evaporated while gently rocking the sample. This method reproducibly results in well-aligned lamellar samples. Samples were then placed under vacuum for ∼2 h to remove traces of solvent. They were then placed into sample holders, sealed, and equilibrated in a humid nitrogen atmosphere at room temperature for several hours. Samples were hydrated at a fixed humidity using a saturated salt solution of KNO_3 (92.3% RH) with 0, 8, 16, and/or 70 mol % ^2H_2O, and kept at room temperature during initial equilibration. During data collection, the external circulating water bath was set to 30.0 ± 0.5 °C, and sample temperature was 28.2 ± 0.5 °C.

Neutron diffraction data were taken using the N5 beamline located at the Canadian Neutron Beam Center (CNBC, Chalk River, Ontario, Canada). A neutron wavelength of 2.37 Å was selected using a single-crystal monochromator. A pyrolytic graphite filter was used to suppress higher-order (i.e., $\lambda/2$, etc.) reflections. Typically, 4−8 quasi-Bragg peaks were observed. The reconstructed unit cell has a canonical resolution of 9−11 Å.

Data correction and reconstruction of the bilayer profile proceeded as outlined in a previous report.[40] The 1D NSLD profile $\rho(z)$ was constructed with the cosine transform of the measured form factors F_h. The difference between labeled and unlabeled data were calculated from measured form factors; $F_h = F_h^{\text{labeled}} - F_h^{\text{unlabeled}}$. Data were placed on an absolute scale by calculating the total SLD of the unit cell, in units of Å^{-2} mol^{-1}.

^{2}H NMR. Pure [$^2H_{31}$]-16:0-18:1PC and 14:0-[$^2H_{27}$]-14:0PC were hydrated from powder (∼50 mg) with an equal weight of 50 mM Tris buffer (pH 7.5) in deuterium-depleted water (DD-water). Prior to hydration, lipid samples containing 10 mol % aToc were first codissolved in $CHCl_3$, which was then removed under argon, and then followed by vacuum pumping for ∼6 h to remove residual traces. All samples were thoroughly mixed with excess DD-water (∼2 mL) to enable pH adjustment and were subsequently lyophilized. Two more rehydrations and lyophilizations with excess DD-water were then performed to remove residual ^{2}HHO. The final samples containing 50 wt % lipid were transferred to 5 mm NMR tubes that were sealed with a Teflon coated plug and stored at −80 °C until NMR experimentation.

NMR spectra were acquired on a home-built spectrometer[51] using a 7.05 T superconducting magnet (Oxford Instruments, Osney Mead, UK) operating at 46.0 MHz and employing a phase alternated quadrupolar echo sequence $(90°_x - \tau - 90°_y - \text{acquire} - \text{delay})_n$.[52] Spectral parameters were 90° pulse width = 3.8 μs; separation between pulses τ = 50 μs; delay between pulse sequences = 0.5 s; sweep width = ± 100 kHz; data set = 2 K; and number of transients = 10000. Powder pattern and depaked spectra were determined from the NMR signal collected. First moments M_1 were calculated with

$$M_1 = \frac{\int_{-\infty}^{\infty} |\omega| f(\omega)\, d\omega}{\int_{-\infty}^{\infty} f(\omega)\, d\omega} \tag{7}$$

where ω is the frequency with respect to the central Larmor frequency ω_o and $f(\omega)$ is the line shape.[23] In practice the integral was a summation over the digitized data.

UV/Vis Oxidation. For pure lipid samples, 1 mg of lipid was hydrated with degassed ultrapure water. Samples containing 10 mol % aToc and/or 0.1 mol % AMVN were codissolved in chloroform, which were then placed under vacuum (1 h) to remove any traces of solvent. Samples were then hydrated with degassed ultrapure water. Lipid suspensions were extruded using a 200 nm pore membrane, and loaded into a quartz cuvette. For external oxidation conditions, the Fenton reagents ($FeSO_4$ and H_2O_2) were added to the lipid dispersion immediately prior to data collection. Oxidation was monitored with an Ultraspec 2100 pro UV/visible spectrophotometer. For internal oxidation conditions, samples containing AMVN were kept at 50 °C (irrespective of lipid species used) in order to have ensured a sufficient rate of radical production. All membranes were in the liquid crystalline phase.

AUTHOR INFORMATION

Corresponding Authors

dm06ti@brockuca
thad.harroun@brockuca

Notes

The authors declare no competing financial interest.

■ ACKNOWLEDGMENTS

We acknowledge the Canadian Neutron Beam Centre (CNBC, Chalk River, ON) for providing generous amounts of neutron beamtime. D.M. is supported by a NSERC Vanier Canada Graduate Scholarship. T.A.H. and J.A. are partially supported by the National Science and Engineering Research Council of Canada (NSERC). J.K. is partially supported from the Laboratory Directed Research and Development Program of Oak Ridge National Laboratory (ORNL), managed by UT-Battelle, LLC, for the U.S. Department of Energy (DOE) under contract no. DE-AC05-00OR2275. Support for J.K. from the Scientific User Facilities Division of the Office of Basic Energy Sciences (BES) is also acknowledged.

■ REFERENCES

(1) Evans, H. M.; Bishop, K. S. *Science* **1922**, *56*, 650−651.
(2) Gohil, K.; Vash, V. T.; Cross, C. E. *Mol. Nutr. Food Res.* **2010**, *54*, 693−709.
(3) Traber, M. G.; Stevens, J. F. *Free Radical Biol. Med.* **2011**, *51*, 1000−1013.
(4) Traber, M. G. *Annu. Rev. Nutr.* **2007**, *27*, 347−362.
(5) Traber, M. G.; Atkinson, J. *Free Radical Biol. Med.* **2007**, *43*, 4−15.
(6) Azzi, A. *Free Radical Biol. Med.* **2007**, *43*, 16−21.
(7) Takahashi, M.; Tsuchiya, J.; Niki, E. *J. Am. Chem. Soc.* **1989**, *111*, 6350−6353.
(8) Serbinova, E.; Kagan, V.; Han, D.; Packer, L. *Free Radical Biol. Med.* **1991**, *10*, 263−275.
(9) Wassall, S.; Wang, L.; McCabe, R.; Ehringer, W.; Stillwell, W. *Chem. Phys. Lipids* **1991**, *60*, 29−37.
(10) Afri, M.; Ehrenberg, B.; Talmon, Y.; Schmidt, J.; Cohen, Y.; Frimer, A. A. *Chem. Phys. Lipids* **2004**, *131*, 107−121.
(11) Fukuzawa, K. *J. Nutr. Sci. Vitaminol.* **2008**, *54*, 273−285.
(12) Tardieu, A.; Luzzati, V.; Reman, F. *J. Mol. Biol.* **1973**, *75*, 711−733.
(13) Katsaras, J.; Tristram-Nagle, S.; Liu, Y.; Headrick, R. L.; Fontes, E.; Mason, P. C.; Nagle, J. F. *Phys. Rev. E* **2000**, *61*, 5668.
(14) Kucerka, N.; Nieh, M.-P.; Katsaras, J. *Biochim. Biophys. Acta* **2011**, *1808*, 2761−2771.
(15) Smith, G. S.; Sirota, E. B.; Safinya, C. R.; Clark, N. A. *Phys. Rev. Lett.* **1988**, *60*, 813−816.
(16) Katsaras, J.; Yang, D. S.-C.; Epand, R. M. *Biophys. J.* **1992**, *63*, 1170.
(17) Raghunathan, V.; Katsaras, J. *Phys. Rev. Lett.* **1995**, *74*, 4456−4459.
(18) Marquardt, D.; Williams, J. A.; Kučerka, N.; Atkinson, J.; Wassall, S. R.; Katsaras, J.; Harroun, T. A. *J. Am. Chem. Soc.* **2013**, *135*, 7523−7533.
(19) Katsaras, J.; Stinson, R.; Davis, J.; Kendall, E. *Biophys. J.* **1991**, *59*, 645−653.
(20) Harroun, T. A.; Katsaras, J.; Wassall, S. R. *Biochemistry* **2006**, *45*, 1227−1233.
(21) Harroun, T. A.; Katsaras, J.; Wassall, S. R. *Biochemistry* **2008**, *47*, 7090−7096.
(22) Kucerka, N.; Liu, Y.; Chu, N.; Petrache, H.; Tristram-Nagle, S.; Nagle, J. *Biophys. J.* **2005**, *88*, 2626−2637.
(23) Davis, J. H. *Biochim. Biophys. Acta* **1983**, *737*, 117−171.
(24) McCabe, M. A.; Wassall, S. R. *Solid State Nucl. Magn. Reson.* **1997**, *10*, 53−61.
(25) J.Suzuki, Y.; Tsuchiya, M.; R.Wassall, S.; Choo, Y. M.; Govil, G.; Kagan, V. E.; Packer, L. *Biochemistry* **1993**, *32*, 10692−10699.
(26) Wassall, S. R.; Thewalt, J. L.; Wong, L.; Gorrissen, H.; Cushley, R. J. *Biochemistry* **1986**, *25*, 319−326.
(27) Lafleur, M.; Fine, B.; Sternin, E.; Cullis, P. R.; Bloom, M. *Biophys. J.* **1989**, *56*, 1037−1041.
(28) Engel, A. K.; Cowburn, D. *FEBS Lett.* **1981**, *126*, 169−171.
(29) Seelig, J. *Q. Rev. Biophys.* **1977**, *10*, 353−418.
(30) Gruen, D. W. R.; Haydon, D. *Biophys. J.* **1981**, *33*, 167−188.
(31) Niki, E. *Methods Enzymol.* **1990**, *186*, 100−108.
(32) Fukuzawa, K.; Gebicki, J. M. *Arch. Biochem. Biophys.* **1983**, *226*, 242−251.
(33) Aussenac, F.; Laguerre, M.; Schmitter, J.-M.; Dufourc, E. J. *Langmuir* **2003**, *19*, 10468−10479.
(34) Jämbeck, J. P. M.; Lyubartsev, A. P. *J. Phys. Chem. B* **2012**, *116*, 3164−3179.
(35) Komljenovic, I.; Marquardt, D.; Harroun, T. A.; Sternin, E. *Chem. Phys. Lipids* **2010**, *163*, 480−487.
(36) Kucerka, N.; Marquardt, D.; Harroun, T. A.; Nieh, M.-P.; Wassall, S. R.; de Jong, D. H.; Schafer, L. V.; Marrink, S. J.; Katsaras, J. *Biochemistry* **2010**, *49*, 7485−7493.
(37) Ruíz-Gutiérrez, V.; Prada, J.; Pérez-Jiménez, F. *J. Chromatogr., B* **1993**, *622*, 117−124.
(38) Fukuzawa, K.; Soumi, K.; Iemura, M.; Goto, S.; Tokumura, A. *Arch. Biochem. Biophys.* **1995**, *316*, 83−91.
(39) Fukuzawa, K.; Matsuura, K.; Tokumura, A.; Suzuki, A.; Terao, J. *Free Radical Biol. Med.* **1997**, *22*, 923−930.
(40) Kucerka, N.; Marquardt, D.; Harroun, T. A.; Nieh, M.-P.; Wassall, S. R.; Katsaras, J. *J. Am. Chem. Soc.* **2009**, *131*, 16358−16359.
(41) Marrink, S. J.; de Vries, A. H.; Harroun, T. A.; Katsaras, J.; Wassall, S. R. *J. Am. Chem. Soc.* **2008**, *130*, 10−11.
(42) Fukuzawa, K.; Ouchi, A.; Shibata, A.; Nagaoka, S.-i.; Mukai, K. *Chem. Phys. Lipids* **2011**, *164*, 205−210.
(43) Fukuzawa, K.; Seko, T.; Minami, K.; Terao, J. *Lipids* **1993**, *28*, 497−503.
(44) Fukuzawa, K.; Chida, H.; Tokumura, A.; Tsukatani, H. *Arch. Biochem. Biophys.* **1981**, *206*, 173−180.
(45) Thomas, C.; McLean, L.; Parker, R.; Ohlweiler, D. *Lipids* **1992**, *27*, 543−550.
(46) Wang, X.-H.; Ushio, H.; Ohshima, T. *Lipids* **2003**, *38*, 65−72.
(47) Aranda, F. J.; Coutinho, A.; Berberan-Santos, M. N.; Prieto, M. J. E.; Gómez-Fernández, J. C. *Biochim. Biophys. Acta* **1989**, *985*, 26−32.
(48) Fukuzawa, K.; Ikebata, W.; Shibata, A.; Kumadaki, I.; Sakanaka, T.; Urano, S. *Chem. Phys. Lipids* **1992**, *63*, 69−75.
(49) Villalain, J.; Aranda, F.; Gomezfernandez, J. *Eur. J. Biochem.* **1986**, *158*, 141−147.
(50) Ekiel, I. H.; Hughes, L.; Burton, G. W.; Jovall, P. A.; Ingold, K. U.; Smith, I. C. P. *Biochemistry* **1988**, *27*, 1432−1440.
(51) Williams, J. A.; Batten, S. A.; Harris, M.; Rockett, B. A.; Shaikh, S. R.; Stillwell, W.; Wassall, S. *Biophys. J.* **2012**, *103*, 228−237.
(52) Davis, J. H.; Jeffrey, K. R.; Bloom, M.; Valic, M. I.; Higgs, T. P. *Chem. Phys. Lett.* **1976**, *42*, 390−394.